Journal of Chromatography A, xxx (2016) xxx–xxx

Contents lists available at ScienceDirect

Journal of Chromatography A

journal homepage: www.elsevier.com/locate/chroma

Methacrylate-bonded covalent-organic framework monolithic columns for high performance liquid chromatography

Li-Hua Liu [a], Cheng-Xiong Yang [a,*], Xiu-Ping Yan [a,b,*]

[a] College of Chemistry, Research Center for Analytical Sciences, State Key Laboratory of Medicinal Chemical Biology, Tianjin Key Laboratory of Molecular Recognition and Biosensing, Nankai University, Tianjin 300071, China
[b] Collaborative Innovation Center of Chemical Science and Engineering (Tianjin), Tianjin 300071, China

ARTICLE INFO

Article history:
Received 17 October 2016
Received in revised form
30 November 2016
Accepted 1 December 2016
Available online xxx

Keywords:
Covalent-organic frameworks
Stationary phase
Monolithic column
High-performance liquid chromatography

ABSTRACT

Covalent-organic frameworks (COFs) are a newfangled class of intriguing microporous materials. Considering their unique properties, COFs should be promising as packing materials for high performance liquid chromatography (HPLC). However, the irregular shape and sub-micrometer size of COFs synthesized via the traditional methods render the main obstacles for the application of COFs in HPLC. Herein, we report the preparation of methacrylate-bonded COF monolithic columns for HPLC to overcome the above obstacles. The prepared COF bonded monolithic columns not only show good homogeneity and permeability, but also give high column efficiency, good resolution and precision for HPLC separation of small molecules including polycyclic aromatic hydrocarbons, phenols, anilines, nonsteroidal anti-inflammatory drugs and benzothiophenes. Compared with the bare polymer monolithic column, the COF bonded monolithic columns show enhanced hydrophobic, π-π and hydrogen bond interactions in reverse phase HPLC. The results reveal the great potential of COF bonded monoliths for HPLC and COFs in separation sciences.

1. Introduction

Covalent organic frameworks (COFs) are a newfangled class of intriguing microporous materials which are constructed from light elements (N, O, B, C, H and Si) and linked with covalent bonds [1–5]. Their unique properties including large surface area, good thermal and solvent stability, low density and accessible pores make them highly promising in wide applications including gas storage [6] catalysis [7,8], photoelectricity [9], and drug delivery [10]. The applications of COFs in separation science have gained increasing concerns recently [11–13]. COFs have been successfully applied as novel stationary phases in high resolution gas chromatography and capillary electrochromatography [11–13]. High performance liquid chromatography (HPLC) is a separation technology widely used in food, chemical, medical and environmental sciences [14]. Considering the intriguing structure and unique properties of COFs, COFs should be promising packing materials for HPLC. However, the COFs synthesized via the traditional methods often show irregular shape or sub-micrometer size, so direct packing of these COFs in HPLC columns may cause low column efficiency and high column backpressure, which are the main obstacles for the application of COFs in HPLC.

Monolithic columns with continuous porous structure not only have the merits of simple synthesis and good stability in a wide pH range, but also give good permeability and rapid mass transfer, which make them promising in fast HPLC separation of large molecules [15–19]. However, the low surface area of polymer monoliths leads to poor efficiency in isocratic separations of small molecules [20]. Incorporation of porous nanoparticles into monolithic materials to fabricate the hybrid monolithic columns has been proved to be an efficient and convenient way to enhance the performance of small molecules separation [21–23]. Recently, porous carbonaceous nanoparticle-based monoliths [24–26], metallic nanoparticle-based monoliths [27,28], silica nanoparticle-based monoliths [29] and metal-organic frameworks-based monoliths [30–33] have been studied for enhanced separation of small molecules.

The combination of the distinctive architecture of polymer monolithic column and the specific merits of COFs is a potential approach to solve the aforementioned problems. On one hand, the incorporation of COFs into polymer monolithic columns reduces the column backpressure and enhances the column efficiency of the COFs packed columns. On the other hand, the incorporated

* Corresponding authors at: College of Chemistry, Research Center for Analytical Sciences, State Key Laboratory of Medicinal Chemical Biology, Tianjin Key Laboratory of Molecular Recognition and Biosensing, Nankai University, Tianjin 300071, China
E-mail addresses: cxyang@nankai.edu.cn (C.-X. Yang), xpyan@nankai.edu.cn, xiupingyan@gmail.com (X.-P. Yan).

http://dx.doi.org/10.1016/j.chroma.2016.12.004
0021-9673/

COFs increase the interaction sites and the surface area of polymer monolithic column.

Herein, we report the synthesis of methacrylate-bonded COF monolithic column not only to overcome the main obstacles for the application of COFs in HPLC, but also to improve the performance of conventional polymer monolithic columns. TpPa-1, synthesized via the aldehyde-amine condensation reaction between the 1, 3, 5-triformylphloroglucinol (Tp) and *p*-phenylenediamine (Pa-1) [34], was used as a typic COF as its good solvent stability and large surface area make TpPa-1 suitable for HPLC. In this work, HPLC separation of small molecules on the methacrylate-bonded COF TpPa-1 monolithic column is achieved with excellent resolution, good precision and high column efficiency.

2. Experimental

2.1. Reagents

All the used reagents were analytical grade at least. 1, 3, 5-triformylphloroglucinoland (Tp) and *meso*-tetra (4-aminophenyl) porphine were purchased from Chengdu Tongchuangyuan pharmaceutical technology Co. (Chengdu, China). Ultrapure water was produced by Tianjin Wahaha Foods Co. (Tianjin, China). Pyrene, naphthalene, chrysene, fluorene, 2-nitroaniline, 2,6-dimethylphenol, acetanilide, aniline, resorcinol, 1-naphthylamine, 2,6-dichlorophenol, 1-naphthol, m-cresol, aspirin, salicylic acid, trifluoroacetic acid (TFA), 2,2′-Azobis(2-methylpropionitrile) (AIBN), ethylene dimethacrylate (EDMA), methyl methacrylate (MMA), methacrylic anhydride (MA), styrene (St), divinylbenzene (DVB), dodecanol, and *p*-phenylenediamine (Pa-1) were produced by Aladdin Chemistry Co. (Shanghai, China). Polyethylene glycol (PEG 6000), ribonuclease A, bovine hemoglobin and myoglobin were bought from Sinopharm Chemical Reagent Co. (Shanghai, China). Thiourea, toluene, chlorobenzene, benzene were from Guangfu Fine Chemical Research Institute (Tianjin, China). Ketoprofen and fenbufen were from Energy Chemical Co. (Shanghai, China). Methanol, ethanol, acetonitrile (ACN), dimethyl sulfoxide (DMSO) and ethyl acetate were from Concord Fine Chemical Research Institute (Tianjin, China).

2.2. Instrumentation

The powder X-ray diffraction spectrometry (PXRD) data were obtained on a D/max-2500 diffractometer (Rigaku, Japan) using CuKα radiation. The Fourier transform infrared spectroscopy (FT-IR) spectra were obtained on the Magna-560 spectrometer (Nicolet, Madison, WI). Scanning electron microscopy (SEM) images and mass spectra were acquired on a Shimadzu SS-550 scanning electron microscope and an Agilent 6520 Q-TOF LC/MS (Agilent, USA), respectively. BET surface areas data were collected on the NOVA 2000e surface area and pore size analyzer (Quantachrome, USA) using N_2 adsorption at 77 K. Nuclear magnetic resonance (NMR) analysis was carried out on the AV400 NMR spectrometer (Bruker, Switzerland). Size distribution was observed on a Zetasizer Nano-ZS (Malvern, UK). Elemental analysis was carried out on a Vario EL CUBE analyzer (Elementary, Germany).

HPLC experiments were performed on Waters 510 HPLC pump fitted with 486 tunable UV detector. An N2000 chromatography data system was applied for data acquisition and processing. Column temperature was controlled by a CO-5060 column heater (Ameritech, USA). The commercial C18 silica gel (Baseline, Tianjin, China) was employed to pack the HPLC column (50.0 mm long × 4.6 mm i.d.) for comparison.

2.3. Synthesis of Tp-MA

MA (184.8 mg, 1.2 mM) and Tp (21.0 mg, 0.1 mM) were separately dissolved in 20 mL THF, and then mixed in a 50 mL flask under stirring at 60 °C. After stirring for 48 h, the product was extracted with ethyl acetate. The obtained extract was dried over $MgSO_4$ and evaporated to give Tp-MA with a yield of 74%. FT-IR (powder): 2983, 1722 and 1115 cm^{-1}. MS (ESI+): 415.10 [M+H]. ^1H NMR (400 MHz $CDCl_3$): 10.15 (s, 3H), 6.25 (s, 3H), 5.69(d, 3H), 1.96 (s, 9H).

2.4. Synthesis of TpPa-MA

Tp-MA (41.4 mg, 0.10 mM) and Pa-1 (16.2 mg, 0.15 mM) were separately dissolved with 20 mL ethanol, then mixed in a 100 mL flask under stirring. After refluxing for 4 h, the light brown suspension was obtained by 5-min centrifugating at 10,000 rpm. The collected brown powder was thoroughly washed with ethanol. The obtained TpPa-MA was dried in vacuum at room temperature overnight to remove ethanol. FT-IR (powder): 1722, 1581, 1448 and 1257 cm^{-1}. PXRD (2 theta): 4.6°, 8.1°, 25.8°.

2.5. Synthesis of poly (TpPa-MA-co-EDMA) monolithic columns

The monomers TpPa-MA and EDMA, and porogen PEG 6000 were dispersed in DMSO via ultrasonication for 2 h to create a homogeneous dispersion. The initiator AIBN was then added and ultrasonicated for 5 min to dissolve AIBN. The obtained polymerization mixture was injected to the stainless-steel column (50.0 mm × 4.6 mm i.d.) with a syringe. The both ends of the stainless-steel column were then sealed. After 24-h polymerization in water bath at 60 °C, the column was washed with methanol to remove unreacted monomer and the porogen. A poly (MMA-co-EDMA) monolithic column prepared in parallel by adding 10.9 mg MMA instead of TpPa-MA dispersion (the molar content of double bonds in MMA is equal to those in TpPa-MA with the concentration of 15 mg mL^{-1}) into polymerization mixture was used for comparison.

2.6. Synthesis of poly (St-co-DVB) monolithic column [35]

St (264 μL) and DVB (174 μL) as monomers, dodecanol (504 μL) as macroporogen, toluene as microporogen (208 μL) and AIBN (10 mg) as initiator were mixed via ultrasonication to create a homogeneous dispersion. The obtained polymerization mixture was injected to the stainless-steel column (50.0 mm × 4.6 mm i.d.) with a syringe. The both ends of the stainless-steel column were sealed. After 24-h polymerization in water bath at 70 °C, the column was washed with acetonitrile to remove the porogen and unreacted monomer.

2.7. Calculation of permeability

The permeability (B_0, m^2) was obtained based on Darcy's Law [36]:

$$B_0 = u\mu L/\Delta P \quad (1)$$

where u, μ, L and ΔP are the superficial velocity of mobile phase ($m\,s^{-1}$), the viscosity of mobile phase (Pa s), the length of the monolithic column (m) and the back pressure of the monolithic column (Pa), respectively.

Please cite this article in press as: L.-H. Liu, et al., Methacrylate-bonded covalent-organic framework monolithic columns for high performance liquid chromatography, J. Chromatogr. A (2016), http://dx.doi.org/10.1016/j.chroma.2016.12.004

2.8. Calculation of thermodynamic parameters

The enthalpy change (ΔH, KJ mol^{-1}), the Gibbs free energy change (ΔG, KJ mol^{-1}) and entropy change (ΔS, J mol^{-1} K^{-1}) for HPLC separation were obtained based on van't Hoff equation [37]:

$$lnk' = -\Delta H/RT + \Delta S/R + ln\Phi \quad (2)$$

$$\Delta G = \Delta H - T\Delta S \quad (3)$$

where k', R, T and Φ are the retention factor, the gas constant, the absolute temperature and the phase ratio, respectively.

$$k' = (t - t_0)/t_0 \quad (4)$$

where t and t_0 are the retention time and the column void time, respectively.

$$\Phi = V_s/V_0 \quad (5)$$

$$V_s = V_{Col} - V_0 \quad (6)$$

$$V_0 = t_0 \times F \quad (7)$$

where V_s, V_0, V_{Col} and F are the volume of the stationary phase, the column void volume, the column's geometrical volume and the mobile phase flow rate, respectively.

3. Results and discussion

3.1. Optimization of preparation condition of poly (TpPa-MA-co-EDMA) monolithic columns

The dispersion of polymerization precursor is a key factor to fabricate the homogeneous nanoparticles-based monolithic columns. In our preliminary experiment, we tried to use a simple mixture of TpPa-1 and the polymerization precursor solution to prepare monolithic columns. However, the poor dispersion of TpPa-1 in the polymerization precursor solution led to inhomogeneous monolithic columns with the use of such simple mixture (Fig. S1). To obtain the homogeneous TpPa-1 monolith column, we prepared the methacrylate-bonded TpPa-1 for subsequent fabrication of poly (TpPa-methacrylic anhydride co-ethylene dimethacrylate) (poly (TpPa-MA-co-EDMA)) monolith (Fig. 1).

The Tp was first reacted with methacrylic anhydride (MA) via esterification to give Tp-MA. The obtained Tp-MA was applied to construct the MA-containing COF TpPa-MA. The TpPa-MA was then added into the polymerization precursor to synthesis poly (TpPa-MA-co-EDMA) monolithic column with improved homogeneity (Fig. S1).

The effects of porogen mass and TpPa-MA concentration on the permeability of poly (TpPa-MA-co-EDMA) monoliths were studied (Table 1). Increase of the porogen content from 230 to 450 mg improved the permeability of poly (TpPa-MA-co-EDMA) monoliths. However, further increase of the porogen content to 560 mg led to no more improvement of the permeability. Therefore, 450 mg of PEG-6000 was used for further experiments. The permeability of poly (TpPa-MA-co-EDMA) monolithic columns increased from 13.2×10^{-15} to 14.9×10^{-15} m^2 as the TpPa-MA concentration increased from 5 to 15 mg mL^{-1}. However, further increase of the TpPa-MA concentration to 20 mg mL^{-1} led to a significant decrease of the permeability, which likely resulted from the aggregation of TpPa-MA nanoparticles at high concentration [32]. Therefore, TpPa-MA concentration of 15 mg mL^{-1} was used for the preparation of poly (TpPa-MA-co-EDMA) monoliths.

3.2. Characterization of Tp-MA, TpPa-MA and poly (TpPa-MA-co-EDMA) monoliths

The synthesized *Tp-MA, TpPa-MA and* poly (TpPa-MA-co-EDMA) monolithic columns were characterized by powder PXRD, FT-IR, SEM, EA, size distribution analysis and N_2 adsorption experiments (Fig. 2; Figs. S2–S9). The appearance of the characteristic bands of C=O at 1722 cm^{-1}, C—O at 1115 cm^{-1} and C—H at 2983 cm^{-1} in the FT-IR spectra of Tp-MA (Fig. S2A) suggests the successful synthesis of Tp-MA. The high-resolution mass spectra (m/z = 414.10) and ^{1}H NMR data (Figs. S3–S5) also confirm all the three —OH groups on Tp were substituted with MA. The characteristic PXRD peaks at 4.6, 8.1 and 25.8 of the as-prepared TpPa-MA well agreed with the simulated pattern (Fig. 2A), indicating the successful synthesis of TpPa-MA. The characteristic FT-IR peaks of C=O stretching at 1722 cm^{-1} also indicate the successful synthesis of TpPa-MA (Fig. 2B). The particle size of TpPa-MA is about 210 nm (Fig. S6). The characteristic PXRD signal of TpPa-MA at 4.6 and 8.1 (Fig. S7) and FT-IR bands of TpPa-MA at 1581, 1448 and 1257 cm^{-1} of poly (TpPa-MA-co-EDMA) (Fig. 2B) confirm that the methacrylate-bonded TpPa-1 monolithic column was successfully prepared (1730 and 1151 cm^{-1} from the poly (MMA-co-EDMA)) (Fig. S2B). The larger surface area of the poly (TpPa-MA-co-EDMA) monolithic column (224 m^2 g^{-1}) than the poly(MMA-co-EDMA) monolithic column (175 m^2 g^{-1}) also demonstrates the successful bonding of TpPa-MA (317 m^2 g^{-1}) into the poly (TpPa-MA-co-EDMA) monolithic column (Fig. S8). SEM images reveal the presence of the TpPa-MA nanoparticles in the monolithic column (Fig. 2C and D; Fig. S9). Elemental analysis shows the ratio of TpPa-MA in poly (TpPa-MA-co-EDMA) monolithic column is about 6.8% (Table S1).

3.3. Enhanced chromatographic separation of small molecules on poly (TpPa-MA-co-EDMA) monoliths

The effect of TpPa-MA concentration on HPLC separation of small molecules from non-polar to polar compounds was studied (Figs. 3 and 4; Table S1). The poly (MMA-co-EDMA) monolithic column (0 mg mL^{-1} of TpPa-MA) gave poor resolution and retention to the tested small molecules. In contrast, the resolution and retention of these small molecules increased with the TpPa-MA concentration (Figs. 3 and 4), showing improved separation on the synthesized poly (TpPa-MA-co-EDMA) monolithic columns. In addition, the poly (TpPa-MA-co-EDMA) monoliths also provided higher column efficiency than the poly (MMA-co-EDMA) monolith without TpPa-MA (Table S2). Increase of the TpPa-MA concentration from 5 to 15 mg mL^{-1} resulted in the increase of the retention, column efficiency and resolution of poly (TpPa-MA-co-EDMA) monolithic columns, which indicates higher TpPa-MA concentration is beneficial for the preparation of poly (TpPa-MA-co-EDMA) monolithic columns (Table S2). However, high TpPa-MA concentration (20 mg mL^{-1}) led to a significant decrease of the permeability (Table 1), which is negative for the application of poly (TpPa-MA-co-EDMA) monolithic column. The difference in column efficiency mainly resulted from the pore size distribution and morphology [38], which can be reflected in the Van Deemter curves (Fig. S10). The three parameters A-term, B-term, and C-term represented eddy dispersion, longitudinal diffusion, and mass transfer resistance, respectively [38]. Compared with poly (MMA-co-EDMA) monolith (0 mg mL^{-1} TpPa-MA) and poly (TpPa-MA-co-EDMA) monoliths (5 and 10 mg mL^{-1} TpPa-MA), poly (TpPa-MA-co-EDMA) monolith (15 mg mL^{-1} TpPa-MA) gave smaller C-term value, which indicates a better mass transfer property between the stationary phase and analytes. Furthermore, the poly (TpPa-MA-co-EDMA) monolithic column (15 mg mL^{-1} TpPa-MA) also showed better permeability and lower back pressure in the flow rate range of 1.0–5.0 mL min^{-1}

Please cite this article in press as: L.-H. Liu, et al., Methacrylate-bonded covalent-organic framework monolithic columns for high performance liquid chromatography, J. Chromatogr. A (2016), http://dx.doi.org/10.1016/j.chroma.2016.12.004

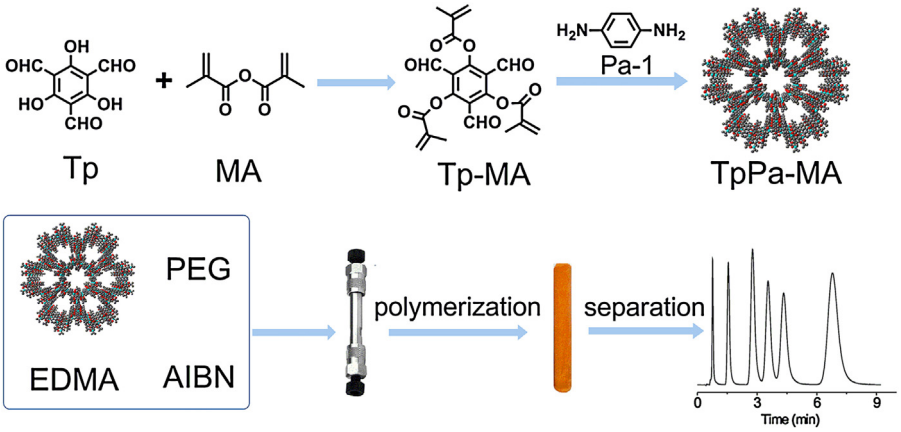

Fig. 1. Schematic illustration for the preparation of the poly (TpPa-MA-co-EDMA) monolith for HPLC.

Table 1
Effect of porogen and TpPa-MA content on the permeability of poly (TpPa-MA-co-EDMA) monoliths.

	Monomers		Porogen	Initiator	
Column	TpPa-MA(mg mL^{-1})	EDMA(μL)	PEG-6000(mg)	AIBN(mg)	Permeability($\times 10^{-15}$ m^2)
1	5	400	230	10	8.14
2	5	400	330	10	11.78
3	5	400	450	10	13.16
4	5	400	560	10	13.20
5	10	400	450	10	13.20
6	15	400	450	10	14.92
7	20	400	450	10	6.30

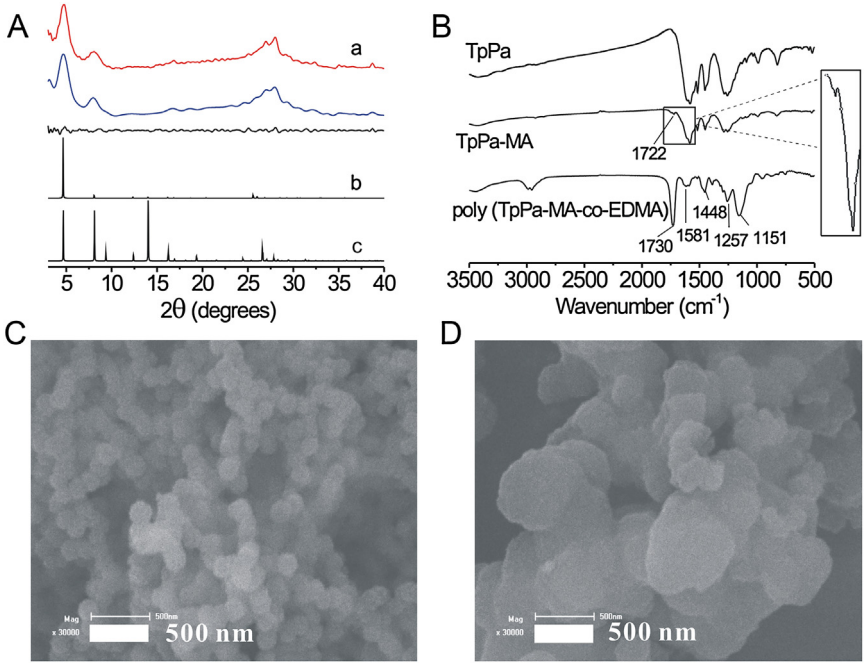

Fig. 2. (A) PXRD patterns of TpPa-MA: (a) Experimental pattern (red curve), refined pattern (blue curve) and the difference plot of the two patterns (black curve). (b) Simulated pattern of the eclipsed model. (c) Simulated pattern of the staggered model. (B) FT-IR spectra of TpPa, TpPa-MA and poly (TpPa-MA-co-EDMA) monolith; (C) SEM image of TpPa-MA; (D) SEM image of poly (TpPa-MA-co-EDMA) monolith. (For interpretation of the references to colour in this figure legend, the reader is referred to the web version of this article.)

than the poly (MMA-co-EDMA) monolith (Fig. S11). These results reveal the significant roles of TpPa-MA in enhanced separation.

The retention of neutral polycyclic aromatic hydrocarbons increased with the aromatic ring number, showing that the retention mechanism resulted from the hydrophobic interaction between the analytes and the TpPa-1 (Fig. 3A). The introduction of the aromatic TpPa-1 into polymer monolithic column increased the hydrophobicity of the stationary phase, thus increased the analyte retention. The retention of thiourea, phenol, benzene, toluene, chlorobenzene and naphthalene decreased as their polarity increased, revealing the reverse-phase chromatographic separation mechanism (Fig. 3B). Thiourea, as the most polar ana-

Please cite this article in press as: L.-H. Liu, et al., Methacrylate-bonded covalent-organic framework monolithic columns for high performance liquid chromatography, J. Chromatogr. A (2016), http://dx.doi.org/10.1016/j.chroma.2016.12.004

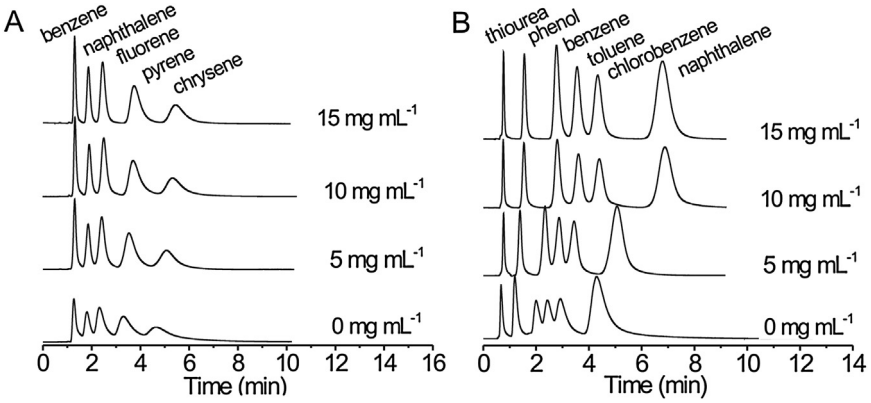

Fig. 3. Effect of TpPa-MA concentration (0, 5, 10, 15 mg mL^{-1}) for the synthesis of poly (TpPa-MA-co-EDMA) monolithic columns (50.0 mm × 4.6 mm i.d.) on the separation: (A) Polycyclic aromatic hydrocarbons using ACN-H_2O (60:40) as the mobile phase at the flow rate of 1.0 mL min^{-1} and UV detection at 254 nm; (B) thiourea, phenol, benzene, toluene, chlorobenzene and naphthalene using ACN-H_2O (40:60) as the mobile phase at the flow rate of 1.0 mL min^{-1} and UV detection at 210 nm.

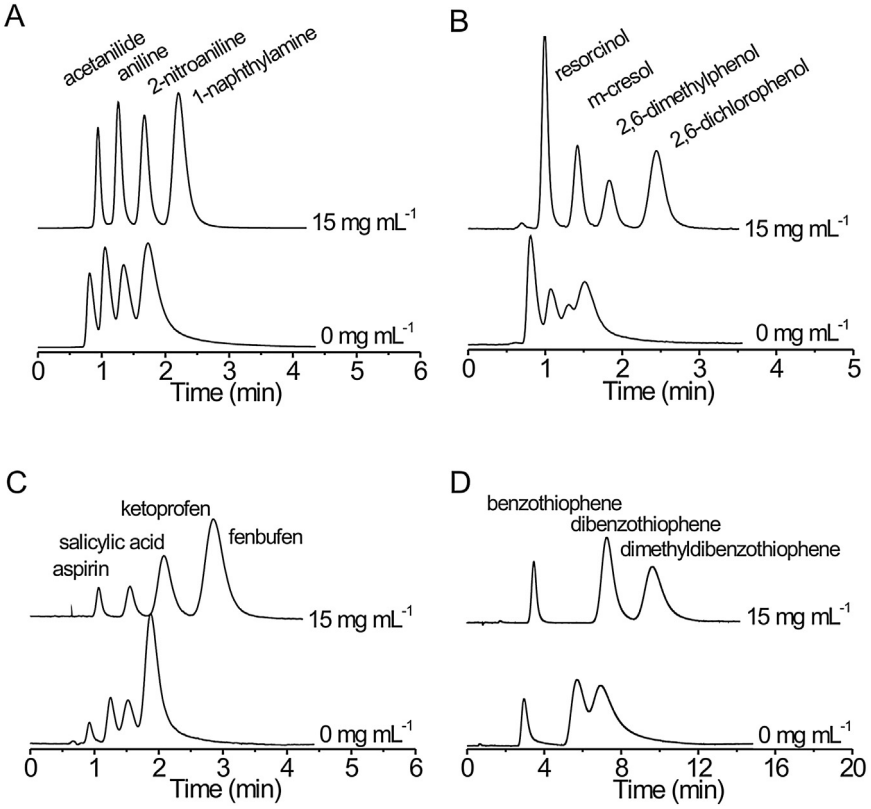

Fig. 4. Separation of (A) basic compounds; (B) acidic compounds; (C) nonsteroidal anti-inflammatory drugs; and (D) benzothiophenes on poly (MMA-co-EDMA) monolithic column (i.e. 0 mg mL^{-1} of TpPa-MA) and poly (TpPa-MA-co-EDMA) monolithic column prepared with 15 mg mL^{-1} of TpPa-MA using ACN-H_2O (50:50) (A, B and D) and ACN-H_2O (45:55) (C) as the mobile phase at a flow rate of 1.0 mL min^{-1} and UV detection at 254 nm (A and D) and 280 nm (B and C).

lyte, was eluted first without retention. The strong retention of naphthalene resulted from the strong hydrophobic interaction between naphthalene and the TpPa-1.

The poly (TpPa-MA-co-EDMA) monolithic column not only showed high resolution for basic compounds, but also for acidic compounds (Fig. 4A and B). Four basic compounds were well separated (Fig. 4A). The retention increased with their basicity. The stronger π-π interaction between the aromatic ring in 1-naphthylamine and the pore walls of TpPa-1 led to stronger retention of 1-naphthylamine than the other three basic compounds. Increase of the hydrophobicity of acidic compounds resulted in the increase of hydrophobic interaction between the acidic compounds and the TpPa-1 (Fig. 4B).

The poly (TpPa-MA-co-EDMA) monolithic column also gave good separation performance for nonsteroidal anti-inflammatory drugs (Fig. 4C) and benzothiophene contaminants (Fig. 4D). Baseline separation was realized on poly (TpPa-MA-co-EDMA) monolithic column due to the hydrophobic interaction and the hydrogen bond interaction between the analytes and TpPa-1. For comparison, the poly (MMA-co-EDMA) monolithic column (without TpPa-MA) gave poor column efficiency and resolution for the separation of all the four groups of small molecule. The above results further underline the enhanced separation performance of the poly (TpPa-MA-co-EDMA) monolithic column.

As the molecular dimensions of the above analytes (Fig. S12) are smaller than the pore size of TpPa-MA (~14 Å) (Fig. S8B), we assume

Please cite this article in press as: L.-H. Liu, et al., Methacrylate-bonded covalent-organic framework monolithic columns for high performance liquid chromatography, J. Chromatogr. A (2016), http://dx.doi.org/10.1016/j.chroma.2016.12.004

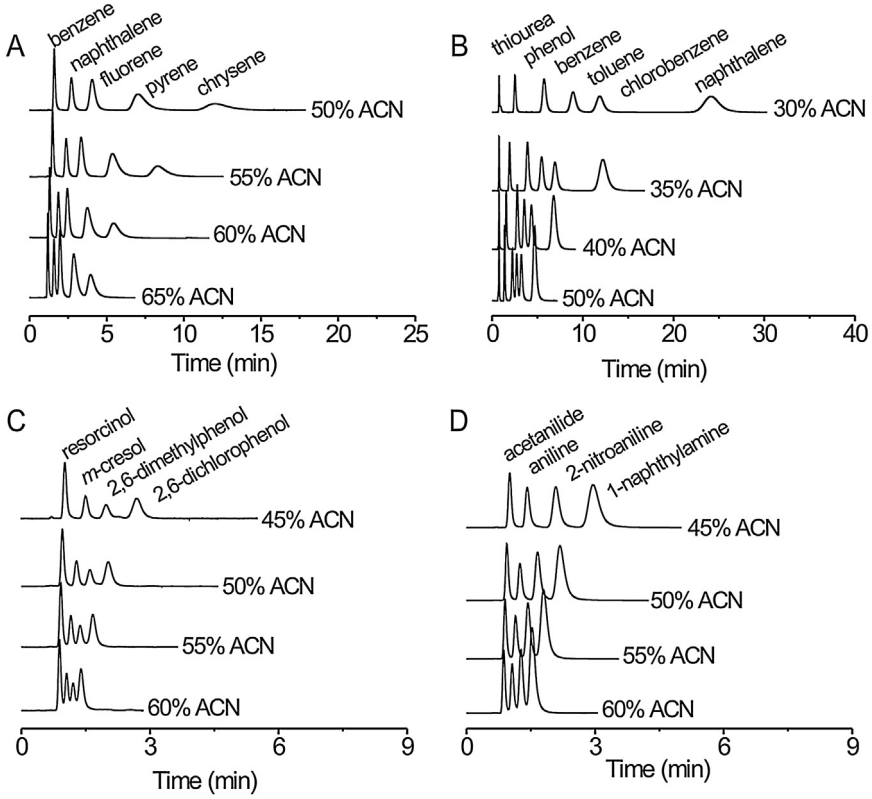

Fig. 5. Effect of ACN content in the mobile phase (ACN-H_2O) on the separation on the poly (TpPa-MA-co-EDMA) monolith (50.0 mm × 4.6 mm i.d.) at a mobile phase flow rate of 1.0 mL min^{-1}: (A) polycyclic aromatic hydrocarbons; (B) thiourea, phenol, benzene, toluene, chlorobenzene, naphthalene; (C) acidic compounds; and (D) basic compounds. UV detection: (A and C) 254 nm, (B) 210 nm, (D) 280 nm.

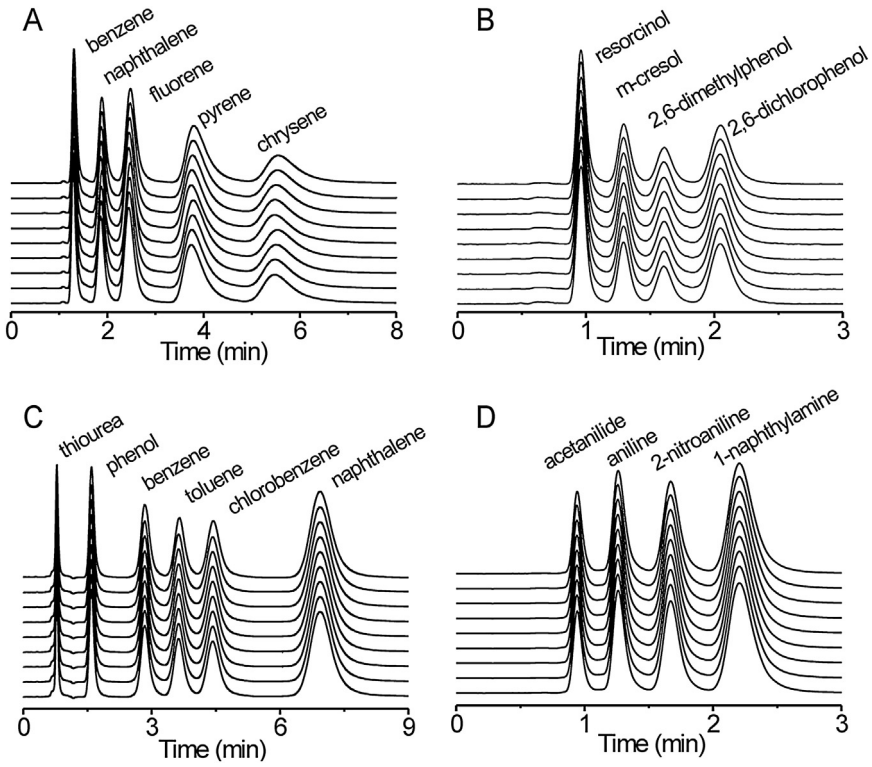

Fig. 6. HPLC chromatograms on the poly (TpPa-MA-co-EDMA) monolith (50.0 mm × 4.6 mm i.d.) at a mobile phase flow rate of 1.0 mL min^{-1} for nine replicate separations: (A) polycyclic aromatic hydrocarbons, (B) acidic compounds, (C) thiourea, phenol, benzene, toluene, chlorobenzene, naphthalene and (D) basic compounds. Mobile phase: (A) ACN-H_2O (60:40), (B) ACN-H_2O (50:50), (C) ACN-H_2O (40:60), (D) ACN-H_2O (50:50). UV detection: (A) 254 nm, (B) 280 nm, (C) 210 nm, (D) 254 nm.

Please cite this article in press as: L.-H. Liu, et al., Methacrylate-bonded covalent-organic framework monolithic columns for high performance liquid chromatography, J. Chromatogr. A (2016), http://dx.doi.org/10.1016/j.chroma.2016.12.004

that the separation of these small molecules mainly occurred inside the pores of TpPa-MA. To further confirm this hypothesis, the *meso*-tetra (4-aminophenyl) porphine (18.5 Å) with the molecule diameter larger than TpPa-MA (~14 Å) was tested (Fig. S13). No retention (0.76 min) of *meso*-tetra (4-aminophenyl) porphine on poly (TpPa-MA-co-EDMA) monolithic column was observed, indicating the size-exclusion effect of TpPa-MA.

The poly (TpPa-MA-co-EDMA) monolithic column (15 mg mL^{-1} TpPa-MA) also gave better resolution than the commercial C_{18} silica gel packed column for the separation of acidic compounds, basic compounds and nonsteroidal anti-inflammatory drugs under the same conditions (Fig. S14; Table S3). The same elution orders for these analytes on poly (TpPa-MA-co-EDMA) monolithic column and C_{18} column (Figs. 3 and 4 *cf.* Fig. S14) further confirms the reverse-phase separation mechanism on poly (TpPa-MA-co-EDMA) monolithic column. Moreover, the poly (TpPa-MA-co-EDMA) monolithic column (15 mg mL^{-1} TpPa-MA) showed better resolution and higher column efficiency than the poly (St-co-DVB) monolithic column [35] for the HPLC separation of these small molecules under the same conditions (Fig. S15). Meanwhile, the poly (TpPa-MA-co-EDMA) monolithic column exhibited faster separation than the metal-organic frameworks-based [30,32] and the functionalized graphene oxide-based [39] monolithic columns and higher column efficiency than the functionalized graphene oxide-based monolithic column (Table S4). In addition, three proteins were baseline separated on the poly (TpPa-MA-co-EDMA) monolithic column (Fig. S16).

3.4. Effect of the composition of mobile phase

The retention and selectivity of the anaiytes decreased with the increase of ACN content in the mobile phase (Fig. 5), indicating the reverse-phase separation mechanism on poly (TpPa-MA-co-EDMA) monolithic column. The analytes were baseline separated on poly (TpPa-MA-co-EDMA) monolithic column by changing the ACN content in the mobile phase. The poly (TpPa-MA-co-EDMA) monolithic column also gave the column efficiency of 20,920 plates m^{-1} for toluene and good precision for nine replicate separations of the tested small molecules with 0.39–3.50%, 0.4–1.92%, 0.06–0.61%, and 0.11–2.09% (relative standard deviations (RSD)) for peak area, peak height, retention time, and half peak width, respectively (Fig. 6 and Table S5).

3.5. Effect of temperature

Effect of temperature (25–55 °C) was studied to obtain an insight into the retention of these tested analytes on the poly (TpPa-MA-co-EDMA) monolithic column (Fig. S17). The retention time of the analytes on the poly (TpPa-MA-co-EDMA) monolithic column decreased remarkably with the increase of column temperature, revealing the separation of these small molecules were exothermic. The peak tailing of these analytes likely resulted from the slow diffusion or mass transfer between the stationary phase and analytes at room temperature. The peak tailing would be improved when increasing the temperature, which was due to higher temperature leading to enhanced diffusion or better mass transfer between the stationary phase and analytes [40]. The good linearity of van't Hoff plots for all the tested small molecules suggests no variation of the interaction mechanism in the studied temperature range (Fig. S18). The negative free energy change (Table S6) shows the thermodynamically spontaneous transfer of the analytes from the mobile phase to the stationary phase. The analytes with more negative free energy change show stronger retention on the poly (TpPa-MA-co-EDMA) monolithic column.

4. Conclusions

In summary, we have prepared novel poly (TpPa-MA-co-EDMA) monolithic columns for enhanced HPLC separation. The poly (TpPa-MA-co-EDMA) monolithic columns not only show good homogeneity and permeability, but also give high column efficiency, good resolution and precision for the separation of small compounds. The good performance of poly (TpPa-MA-co-EDMA) monolithic columns for HPLC separation relies on the hydrophobic, π-π, and hydrogen bond interaction between analytes and the TpPa-1. These results suggest the poly (TpPa-MA-co-EDMA) monolithic columns offer great potential for HPLC separation.

Acknowledgements

XPY appreciates the support from the National Basic Research Program of China (Grant 2015CB932001), National Natural Science Foundation of China (Grant 21305071), Tianjin Natural Science Foundation (Grants 14JCZDJC37600 and 14JCQNJC06600).

Appendix A. Supplementary data

Supplementary data associated with this article can be found, in the online version, at http://dx.doi.org/10.1016/j.chroma.2016.12.004.

References

[1] A. P.Côté, A.I. Benin, N.W. Ockwig, M. O'Keeffe, A.J. Matzger, O.M. Yaghi, Porous, crystalline, covalent organic frameworks, Science 310 (2005) 1166–1170.
[2] X. Feng, X.-S. Ding, D.-L. Jiang, Covalent organic frameworks, Chem. Soc. Rev. 41 (2012) 6010–6022.
[3] S.-S. Han, J.L. Mendoza-Cortes, W.A. Goddard III, Recent advances on simulation and theory of hydrogen storage in metal-organic frameworks and covalent organic frameworks, Chem. Soc. Rev. 38 (2009) 1460–1476.
[4] P.J. Waller, F. Gándara, O.M. Yaghi, Chemistry of covalent organic frameworks, Acc. Chem. Res. 48 (2015) 3053–3063.
[5] U. Díaz, A. Corma, Coord. ordered covalent organic frameworks, COFs and PAFs from preparation to application, Chem. Rev. 311 (2016) 85–124.
[6] S.S. Han, H. Furukawa, O.M. Yaghi, W.A. Goddard III, Covalent organic frameworks as exceptional hydrogen storage materials, J. Am. Chem. Soc. 130 (2008) 11580–11581.
[7] H. Xu, X. Chen, J. Gao, J.-B. Lin, M. Addicoat, S. Irle, D.-L. Jiang, Catalytic covalent organic frameworks via pore surface engineering, Chem. Commun. 50 (2014) 1292–1294.
[8] Q.-R. Fang, S. Gu, J. Zheng, Z.-B. Zhuang, S.-L. Qiu, Y.-S. Yan, 3D Microporous base-functionalized covalent organic frameworks for size-selective catalysis, Angew. Chem. Int. Ed. 53 (2014) 2878–2882.
[9] M. Dogru, T. Bein, On the road towards electroactive covalent organic frameworks, Chem. Commun. 50 (2014) 5531–5546.
[10] Q.-R. Fang, J.-H. Wang, S. Gu, R.B. Kaspar, Z.-B. Zhuang, J. Zheng, H.-X. Guo, S.-L. Qiu, Y.-S. Yan, 3D porous crystalline polyimide covalent organic frameworks for drug delivery, J. Am. Chem. Soc. 137 (2015) 8352–8355.
[11] C.-X. Yang, C. Liu, Y.-M. Cao, X.-P. Yan, Facile room-temperature solution-phase synthesis of a spherical covalent organic framework for high-resolution chromatographic separation, Chem. Commun. 51 (2015) 12254–12257.
[12] H.-L. Qian, C.-X. Yang, X.-P. Yan, Bottom-up synthesis of chiral covalent organic frameworks and their bound capillaries for chiral separation, Nat. Commun. 7 (2016) 12104–12111.
[13] X.-Y. Niu, S.-Y. Ding, W.-F. Wang, Y.-L. Xu, Y.-Y. Xu, H.-L. Chen, X.G. Chen, Separation of small organic molecules using covalent organic frameworks-LZU1 as stationary phase by open-tubular capillary electrochromatography, J. Chromatogr. A 1436 (2016) 109–117.
[14] S. Ahuja, Chromatography and Separation Science, Elsevier Science, USA, 2003.
[15] M.-H. Wu, R.-A. Wu, R.-B. Li, H.-Q. Qin, J. Dong, Z.-B. Zhang, H.-F. Zou, Polyhedral oligomeric silsesquioxane as a cross-linker for preparation of inorganic-organic hybrid monolithic columns, Anal. Chem. 82 (2010) 5447–5454.
[16] H. Lin, J.-J. Ou, Z.-B. Zhang, J. Dong, M.-H. Wu, H.-F. Zou, Facile preparation of zwitterionic organic-silica hybrid monolithic capillary column with an improved one-pot approach for hydrophilic-interaction liquid chromatography (HILIC), Anal. Chem. 84 (2012) 2721–2728.

Please cite this article in press as: L.-H. Liu, et al., Methacrylate-bonded covalent-organic framework monolithic columns for high performance liquid chromatography, J. Chromatogr. A (2016), http://dx.doi.org/10.1016/j.chroma.2016.12.004

[17] M.-L. Chen, L.-M. Li, B.-F. Yuan, Q. Ma, Y.-Q. Feng, Preparation and characterization of methacrylate-based monolith for capillary hydrophilic interaction chromatography, J. Chromatogr. A 1230 (2012) 54–60.
[18] S. Karenga, Z. El Rassi, Neutral Hydroxylated octadecyl acrylate monolith with fast electroosmotic flow velocity and its application to the separation of various solutes including peptides and proteins in the absence of electrostatic interactions, Electrophoresis 31 (2010) 3192–3199.
[19] Z.-S. Liu, J.-J. Ou, H. Lin, H.-W. Wang, Z.-Y. Liu, J. Dong, H.-F. Zou, Preparation of monolithic polymer columns with homogeneous structure via photoinitiated thiol-yne click polymerization and their application in separation of small molecules, Anal. Chem. 86 (2014) 12334–12340.
[20] I. Nischang, I. Teasdale, O. Brüggemann, Porous polymer monoliths for small molecules separations: advancements and limitations, Anal. Biol. Chem. 400 (2010) 2289–2304.
[21] S. Tang, Y. Guo, C.-M. Xiong, S.-J. Liu, X. Liu, S.-X. Jiang, Nanoparticle-based monoliths for chromatographic separations, Analyst 139 (2014) 4103–4117.
[22] F.-G. Ye, S. Wang, S.-L. Zhao, Preparation and characterization of mixed-mode monolithic silica column for capillary electrochromatography, J. Chromatogr. A 1216 (2009) 8845–8850.
[23] P. Zhang, J.-N. Wang, H.-G. Yang, L.-J. Su, Y.-H. Xiong, F.-G. Ye, Facile one-pot preparation of chiral monoliths with a well-defined framework based on the thiol-ene click reaction for capillary liquid chromatography, RSC Adv. 6 (2016) 24835–24842.
[24] Y. Li, Y. Chen, R. Xiang, D. Ciuparu, L.D. Pfefferle, C. Horváth, J.A. Wilkins, Incorporation of single-wall carbon nanotubes into an organic polymer monolithic stationary phase for μ-HPLC and capillary electrochromatography, Anal. Chem. 77 (2005) 1398–1406.
[25] S.D. Chambers, F. Svec, J.M.J. Fréchet, Incorporation of carbon nanotubes in porous polymer monolithic capillary columns to enhance the chromatographic separation of small molecules, J. Chromatogr. A 1218 (2011) 2546–2552.
[26] M.-M. Wang, X.-P. Yan, Fabrication of graphene oxide nanosheets incorporated monolithic column via one-step room temperature polymerization for capillary electrochromatography, Anal. Chem. 84 (2012) 39–44.
[27] K.-J. Yao, J.-X. Yun, S.-C. Shen, L.-H. Wang, X.-J. He, L.-M. Yu, Characterization of a novel continuous supermacroporous monolithic cryogel embedded with nanoparticles for protein chromatography, J. Chromatogr. A 1109 (2006) 103–110.
[28] Z. Zajickova, E. Rubi, F. Svec, In situ sol-gel preparation of porous alumina monoliths for chromatographic separations of adenosine phosphates, J. Chromatogr. A 1218 (2011) 3555–3558.
[29] Y.-X. Liu, Y.-Z. Chen, H.-H. Yang, L.-H. Nie, S.-Z. Yao, Cage-like silica nanoparticles-functionalized silica hybrid monolith for high performance capillary electrochromatography via one-potprocess, J. Chromatogr. A 1283 (2013) 132–139.
[30] Y.-Y. Fu, C.-X. Yang, X.-P. Yan, Incorporation of metal-organic framework UiO-66 into porous polymer monoliths to enhance the liquid chromatographic separation of small molecules, Chem. Commun. 49 (2013) 7162–7164.
[31] L.-M. Li, F. Yang, H.-F. Wang, X.-P. Yan, Metal-organic framework polymethyl methacrylate composites for open-tubular capillary electrochromatography, J. Chromatogr. A 1316 (2013) 97–103.
[32] S.-C. Yang, F.-G. Ye, Q.-H. Lv, C. Zhang, S.-F. Shen, S.-L. Zhao, Incorporation of metal-organic framework HKUST-1 into porous polymer monolithic capillary columns to enhance the chromatographic separation of small molecules, J. Chromatogr. A 1360 (2014) 143–149.
[33] S.-C. Yang, F.-G. Ye, C. Zhang, S.-F. Shen, S.-L. Zhao, In situ synthesis of metal–organic frameworks in a porous polymer monolith as the stationary phase for capillary liquid chromatography, Analyst 140 (2015) 2755–2761.
[34] B.P. Biswal, S. Chandra, S. Kandambeth, B. Lukose, T. Heine, R. Banerjee, Mechanochemical synthesis of chemically stable isoreticular covalent organic frameworks, J. Am. Chem. Soc. 135 (2013) 5328–5331.
[35] I. Nischang, I. Teasdale, O. Brüggemann, Towards porous polymer monoliths for the efficient, retention-independent performance in the isocratic separation of small molecules by means of nano-liquid chromatography, J. Chromatogr. A 1217 (2010) 7514–7522.
[36] C. Martin, J. Coyne, G. Carta, Properties and performance of novel high-resolution/high-permeability ion-exchange media for protein chromatography, J. Chromatogr. A 1069 (2005) 43–52.
[37] M. Śliwka-Kaszyńska, K. Jaszczołt, D. Witt, J. Rachoń, Highperformance liquid chromatography of Di-and trisubstituted aromatic positional isomers on 1, 3-alternate 25, 27-dipropoxy-26, 28-bis-[3-propyloxy]-calix [4] arene-bonded silica gel stationary phase, J. Chromatogr. A 1055 (2004) 21–28.
[38] H.-Y. Zhang, J.-J. Ou, Z.-S. Liu, H.-W. Wang, Y.-M. Wei, H.-F. Zou, Preparation of hybrid monolithic columns via one-pot photoinitiated thiol-acrylate polymerization for retention-independent performance in capillary liquid chromatography, Anal. Chem. 87 (2015) 8789–8797.
[39] Y.-P. Li, L. Qi, H.-M. Ma, Preparation of porous polymer monolithic column using functionalized graphene oxide as a functional crosslinker for high performance liquid chromatography separation of small molecules, Analyst 138 (2013) 5470–5478.
[40] H.-Y. Liu, X.-M. Bai, D. Wei, G.-L. Yang, High-performance liquid chromatography separation of small molecules on a porous poly (trimethylol propane triacrylate-co-N-isopropylacrylamide-co-ethylene dimethacrylate) monolithic column, J. Chromatogr. A 1324 (2014) 128–134.

Please cite this article in press as: L.-H. Liu, et al., Methacrylate-bonded covalent-organic framework monolithic columns for high performance liquid chromatography, J. Chromatogr. A (2016), http://dx.doi.org/10.1016/j.chroma.2016.12.004